

**2-D RESISTIVITY, MAGNETIC AND GPR
SIGNATURE TOWARDS HUMAN BURIALS
AFFECTED BY TEMPORAL VARIATION AND
TYPE OF SOIL**

MUHAMAD HAFIZUDDIN BIN MOHD MANSOR

UNIVERSITI SAINS MALAYSIA

2019

**2-D RESISTIVITY, MAGNETIC AND GPR
SIGNATURE TOWARDS HUMAN BURIALS
AFFECTED BY TEMPORAL VARIATION AND
TYPE OF SOIL**

by

MUHAMAD HAFIZUDDIN BIN MOHD MANSOR

**Thesis submitted in fulfilment of the requirements
for the degree of
Master of Science**

March 2019

ACKNOWLEDGEMENT

First and foremost, praise to Allah for His mercy for giving me this opportunity to further study in Master's degree. I would like to express my sincere gratitude to my supervisor, Dr Nur Azwin Ismail for the continuous support of my master project, for her patience, motivation, enthusiasm and immense knowledge. Her guidance helped me in all the time of research and writing of this thesis. One simply could not wish for a better or friendlier supervisor.

My sincere thanks also goes to Geophysics lecturers and Geophysics lab staff for sacrificing their time and energy assisting me in the projects.

I would like to thank to my geophysics team Mr Muhammad Iqbal Mubarak Faharul Azman, Mr Azim Hilmy Mohamad Yusof and Ms Najmiah Rosli for helping me in data acquisition. My deepest gratitude to the other postgraduate students Nordiana Ahmad Nawawi, Hazrul Hisham Badrul Hisham, Umi Maslinda Anuar, Muhamad Afiq Saharudin, Muhammad Taquiuddin Zakaria, Nur Amalina Mohd Khoirul Anuar, Nurina Auni Ismail, Mohd Hanis Mohamad, Mr Johari Jusoh and others for the motivation and support throughout my master journey

Further and the most important, million thanks to my family; my parents Mohd Mansor Safiee and Halimah Taib and my siblings Muhd Helmi Mansor and Noorashikin Mansor for their prayers, support and understanding during my study.

In addition, I would like to thank to the Centre for Global Archaeological Research (CGAR) of USM staff Mr Shyeh Sahibul Karamah Masnan for helping in this study. A highly thank to short term grant 304/PFIZIK/6315022. Finally, I would like to thank USM Fellowship Scheme for providing fund during my study.

TABLE OF CONTENTS

ACKNOWLEDGEMENT	ii
TABLE OF CONTENTS	iii
LIST OF TABLES	vii
LIST OF FIGURES	viii
LIST OF SYMBOLS	xii
LIST OF ABBREVIATIONS	xiv
ABSTRAK	xvi
ABSTRACT	xviii
CHAPTER 1 INTRODUCTION	1
1.1 Preface	1
1.2 Problem statement	2
1.3 Objective	3
1.4 Scope of study	3
1.5 Significant of study	4
1.6 Layout of thesis	4
CHAPTER 2 LITERATURE REVIEW	6
2.1 Introduction	6
2.2 2-D resistivity	7
2.2.1 Pole dipole electrode array	9
2.3 Ground Penetrating Radar (GPR).....	10
2.3.1 Reflectivity	11
2.4 Magnetic	13
2.4.1 Proton precession magnetometer	13
2.4.2 Filtering	15
2.5 Temporal variation	16

2.6	Effect of different types of soil	23
2.7	Rate of decomposition.....	28
2.8	Chapter summary	30
CHAPTER 3 METHODOLOGY		32
3.1	Introduction	32
3.2	Geology and geomorphology of study area	34
3.2.1	Permatang Pasir.....	34
3.2.2	Titi Teras	35
3.2.3	Nibong Tebal.....	36
3.2.4	Permatang Tok Jaya	37
3.3	Procedure.....	38
3.3.1	Particle size distribution (PSD) analysis	38
3.3.1(a)	Experiment procedure	39
3.3.1(b)	Coefficient of curvature, Cc and Coefficient of uniformity, Cu.....	40
3.3.2	2-D resistivity method.....	42
3.3.3	Ground Penetrating Radar (GPR) method	43
3.3.4	Magnetic method.....	44
3.4	Data acquisition.....	45
3.4.1	Permatang Pasir.....	45
3.4.2	Titi Teras	46
3.4.3	Nibong Tebal.....	48
3.4.4	Permatang Tok Jaya	49
3.5	Data processing	50
3.5.1	2-D resistivity.....	50
3.5.2	Ground Penetrating Radar (GPR)	51
3.5.3	Magnetic.....	52
3.6	Burial age classification	52

3.7	Chapter summary	53
CHAPTER 4 RESULT AND DISCUSSION		54
4.1	Introduction	54
4.2	Result and discussion	54
4.2.1	Permatang Pasir.....	54
4.2.1(a)	PSD analysis.....	55
4.2.1(b)	2-D resistivity survey	56
4.2.1(c)	Ground Penetrating Radar	61
4.2.1(d)	Magnetic.....	66
4.2.1(e)	3D analysis of resistivity and GPR	69
4.2.1(f)	Correlation between geophysical method	71
4.2.2	Titi Teras	73
4.2.2(a)	PSD analysis.....	73
4.2.2(b)	2-D resistivity.....	74
4.2.2(c)	GPR survey	79
4.2.2(d)	Magnetic.....	83
4.2.2(e)	3-D analysis of 2-D resistivity and GPR.....	85
4.2.2(f)	Correlation of geophysical methods.....	87
4.2.3	Nibong Tebal.....	90
4.2.3(a)	2-D resistivity survey	90
4.2.3(b)	GPR survey	95
4.2.3(c)	Magnetic survey	95
4.2.3(d)	3D analysis of resistivity.....	99
4.2.3(e)	Excavation.....	100
4.2.4	Permatang Tok Jaya	101
4.2.4(a)	PSD analysis.....	102
4.2.4(b)	2D resistivity survey.....	104
4.2.4(c)	GPR survey	105
4.2.4(d)	Magnetic survey	107
4.3	Analysis of signature based on time of burials and type of soils	107
4.4	Chapter summary	113
CHAPTER 5 CONCLUSION AND RECOMMENDATIONS.....		114
5.1	Conclusion.....	114

5.2	Recommendations for future research.....	115
	REFERENCES.....	116
	APPENDICES	120

LIST OF TABLES

	Page
Table 2.1	Bulk dielectric constants of common earth materials (Cardimona, 2002). 12
Table 2.2	Summary of GPR and bulk resistivity in contrasting type of soils (Hansen et al. 2014). 24
Table 2.3	Summary of geophysical method in contrasting soil (Pringle et al. 2012b). 25
Table 3.1	Name of equipment as labelled in Figure 3.6. 39
Table 3.2	Summary of soil classification (Santamarina et al., 2001)..... 41
Table 4.1	The summary of PSD analysis. 56
Table 4.2	Summary of burial detection by 2-D resistivity survey. 61
Table 4.3	Summary of burial detection by GPR survey. 66
Table 4.4	Depth of burials by Euler deconvolution. 68
Table 4.5	Summary of PSD analysis calculation. 74
Table 4.6	Summary of burial detection by 2-D resistivity survey. 78
Table 4.7	Summary of burial detection by GPR survey. 82
Table 4.8	Depth of burials by Euler deconvolution. 85
Table 4.9	Summary of PSD analysis calculation. 103
Table 4.10	Classification of burials in consideration of type of soil and age of burials. 108
Table 4.11	Dielectric constant for reflectivity coefficient calculation..... 110
Table 4.12	Final information of GPR and resistivity result of burials. 112

LIST OF FIGURES

	Page
Figure 2.1	Current flow in homogenous ground (Milson, 2007). 7
Figure 2.2	Arrangement of electrodes (Milson, 2007). 8
Figure 2.3	Simplified diagram of (A) the constituents of a radar system with (B) the interpreted section (Reynolds, 2011). 11
Figure 2.4	The concept of proton precession magnetometer where a) the elements of proton precession magnetometer, b) current in magnetizing coil produces a strong field that aligns the magnetic moments and c) the proton spins precess about the geomagnetic field inducing an alternating current in the coil (Lowrie, 2007). 14
Figure 2.5	Result of processed and normalised resistivity survey (a) 28 days after burials (b) 140 days after burial (c) 192 days after burial (d) 252 days after burial (e) 364 days after burial. The edges of each graves are marked by red box (Jervis et al. 2009). 17
Figure 2.6	Bulk ground resistivity data over simulated clandestine graves. a) location of burials, b) resistivity data result (Pringle and Jervis, 2010). 18
Figure 2.7	Processed bulk ground resistivity plan view where the red box indicates the potential burials location (Pringle and Jervis, 2010). ... 19
Figure 2.8	GPR 2D profile for 110, 225 and 450 MHz in 12, 24, 36, 48 and 60 months after burials (Booth and Pringle, 2016). 20
Figure 2.9	Result of geophysical methods which are a) map of resistivity distribution, b) detailed elaboration of vertical derivative of magnetic induction vector medolus, c) map of graves and pits and d) excavation result of a grave (Epov et al. 2016). 21
Figure 2.10	Electrical resistivity tomograms (Büyüksaraç et al. 2016). 22
Figure 2.11	2D GPR profile (Büyüksaraç et al. 2016). 23
Figure 2.12	Analytic signal of the anomaly marked with white dotted (Büyüksaraç et al. 2016). 23

Figure 2.13	2D GPR profile for study cases by using 250 MHz antenna (Molina et al. 2015).....	26
Figure 2.14	Electrical resistivity and magnetic susceptibility of simulated graves (Molina et al. 2015).	27
Figure 2.15	Information of decomposition stages and time frame (Wilson et al. 2007).....	29
Figure 2.16	Decomposition process of a body in open air and closed structure (Galloway et al. 1989).....	30
Figure 3.1	Flow chart of the research.	33
Figure 3.2	Study area at Muslim cemetery of Kampung Permatang Pasir (Google earth pro, 2018)	35
Figure 3.3	Study area at Kampung Titi Teras Muslim cemetery (Google earth pro, 2018).	36
Figure 3.4	Study area at Kampung Tokang, Nibong Tebal (Google earth pro, 2018).	37
Figure 3.5	Study area of Kampung Permatang Tok Jaya (Google earth pro, 2018).	38
Figure 3.6	Instrument for PSD analysis.	39
Figure 3.7	Survey lines at Permatang Pasir Muslim cemetery.....	46
Figure 3.8	Layout of observed grave in Permatang Pasir Muslim cemetery.	46
Figure 3.9	Survey line at Titi Teras Muslim cemetery.....	47
Figure 3.10	Layout of observed grave in Titi Teras Muslim cemetery.	48
Figure 3.11	Survey lines at Nibong Tebal.	49
Figure 3.12	Survey line at Permatang Tok Jaya.	50
Figure 4.1	Observed graves layout at Permatang Pasir Muslim cemetery.....	55
Figure 4.2	PSD analysis graph for Permatang Pasir.....	56
Figure 4.3	Resistivity section of a) RPP1, b) RPP2 and c) RPP3.	58
Figure 4.4	Resistivity section of a) RPP4, b) RPP5 and c) RPP6.	59
Figure 4.5	Resistivity section of a) RPP7, b) RPP8 and c) RPP9.	60
Figure 4.6	Radagram of GPR survey for a) GPP1 and b) GPP2.....	63
Figure 4.7	Radagram of GPR survey for a) GPP3 and b) GPP4.....	63
Figure 4.8	Radagram of GPR survey for a) GPP5 and b) GPP6.....	64
Figure 4.9	Radagram of GPR survey for a) GPP7 and b) GPP8.....	65
Figure 4.10	Radagram of GPR survey GPP9.....	65

Figure 4.11	Magnetic countour map at Permatang Pasir.....	67
Figure 4.12	Analytic signal contour map at Permatang Pasir.	68
Figure 4.13	Euler deconvolution on analytic signal contour map.....	68
Figure 4.14	Depth slice for resistivity survey at depth of a) 1.1 m and b) 1.3 m.....	70
Figure 4.15	The GPR slice at depth a) 1.1 m and b) 1.3 m.	71
Figure 4.16	Correlation between a) the sketch of observed grave, b) analytic signal contour map overlayed by observed graves, c) 1.1 m and 1.3 m GPR depth slice and d) 1.1 m resistivity depth slice.	72
Figure 4.17	Observed graves layout at Titi Teras Muslim cemetery.	73
Figure 4.18	PSD analysis graph for Titi Teras study area.....	74
Figure 4.19	Resistivity section of a) RTT1, b) RTT2 and c) RTT3.....	75
Figure 4.20	Resistivity section of a) RTT4, b) RTT5 and c) RTT6.....	77
Figure 4.21	Resistivity section of a) RTT7, b) RTT8 and c) RTT9.....	78
Figure 4.22	Radagram for GPR survey a) GTT1 and b) GTT 2.	80
Figure 4.23	Radagram for GPR survey a) GTT3 and b) GTT4.	81
Figure 4.24	Radagram for GPR survey a) GTT5 and b) GTT6.	81
Figure 4.25	Radagram for GPR survey a) GTT7 and b) GTT8.	82
Figure 4.26	Radagram for GPR survey GTT9.	82
Figure 4.27	Magnetic contour map at Titi Teras.	83
Figure 4.28	Analytic signal contour map at Titi Teras.....	84
Figure 4.29	Location and depth of point of interest by Euler deconvolution.....	85
Figure 4.30	Resistivity depth slice at a) 0.9 m and b) 1.1 m.	86
Figure 4.31	GPR depth slice at a) 0.9 m and b) 1.1 m.	87
Figure 4.32	Correlation between a) layout of observed graves on the surface, b) analytic signal contour map overlayed observed graves, c) 0.9 m GPR depth slice and d) 0.9 m resistivity depth slice.	89
Figure 4.33	Resistivity section at a) RNT1, b) RNT2 and c) RNT3.....	91
Figure 4.34	Resistivity section at a) RNT4, b) RNT5 and c) RNT6.	92
Figure 4.35	Resistivity section at a) RNT7, b) RNT8 and c) RNT9.....	93
Figure 4.36	Resistivity section at a) RNT10 and b) RNT11.	94
Figure 4.37	Total magnetic field contour map at Nibong Tebal.	97
Figure 4.38	Analytic signal contour map at Nibong Tebal.	98
Figure 4.39	Depth estimated by Euler deconvolution.	99

Figure 4.40	Resistivity depth slice at a) 0.9 m and b) 1.1 m.	100
Figure 4.41	Excavation in study area where a) the location of discovered skeleton and b) the almost complete set of excavated skeleton.	101
Figure 4.42	The discovered of a skull a) on the surface and b) the skull after cleaned.....	101
Figure 4.43	Layout of graves in Permatang Tok Jaya study area.....	102
Figure 4.44	PSD analysis graph for Permatang Tok Jaya.	103
Figure 4.45	The situation during excavation.	103
Figure 4.46	Resistivity section of a) Line 1 and b) Line 2.	104
Figure 4.47	GPR survey lines for a) GPTJ1 and b) GPTJ2.....	105
Figure 4.48	GPR survey lines for a) GPTJ3 and b) GPTJ4.....	106
Figure 4.49	GPR survey lines for a) GPTJ5, b) GPTJ6, c) GPTJ7 and d) GPTJ8.....	107
Figure 4.50	Resistivity values of burials varies in time and type of soil.....	109
Figure 4.51	GPR reflectivity coefficient of burials varies in time and type of soils.	110

LIST OF SYMBOLS

A	Cross-sectional area
a	Spacing between P ₁ and P ₂
B _e	Original alignment of earth magnetic field
c	Speed of light
C _c	Curvature coefficient
C _u	Uniformity coefficient
D ₆₀	diameter corresponding to 60 % finer
D ₃₀	diameter corresponding to 30 % finer
D ₁₀	diameter corresponding to 10 % finer
$\frac{d}{dx} / \frac{d}{dy}$	Horizontal derivative
$\frac{d}{dz}$	Vertical derivative
F	Total magnetic field
f	Frequency
I	Current
k	Geometric factor
L	Length
m	Meter
m/ns	Speed in nanoseconds
N	Structural index
n	Spacing from current electrode
R	Resistance
V	Voltage
v	Velocity
x ₀ , y ₀ and z ₀	Source location of magnetic field

$ A(x,y) $	Analytic signal
ϵ_0	Dielectric permittivity in free space
ϵ_r	Dielectric permittivity of a material
ϵ	Dielectric permittivity constant
Ωm	Ohm meter
ρ	Resistivity
ρ_a	Apparent resistivity
ω	Angular frequency
π	3.42222222
f	Precession frequency
γ_p	Gyromagnetic ratio of proton
%	Percentage

LIST OF ABBREVIATIONS

2D	Two dimensions
3D	Three dimensions
AD	Anno Domini
A	Anomaly
ASTM	America Society for Testing and Materials
BC	Before Christ
C ₁ /C ₂	Current electrode
DC	Direct Current
E	East
EM	Electromagnetic
ERT	Electrical Resistivity Tomography
G	Grave
GPP	GPR Permatang Pasir
GPR	Ground Penetrating Radar
GPS	Global Positioning System
GPTJ	GPR Permatang Tok Jaya
GTT	GPR Titi Teras
MHz	Mega Hertz
MI	Magnetic imaging
N	North
NW	North-west
P	Pipe
P ₁ /P ₂	Potential electrode
ppm	Part per million
PSD	Particle Size Distribution
R _c	Reflectivity coefficient
RMS	Root Mean Square
RNT	Resistivity Nibong Tebal
RPP	Resistivity Permatang Pasir
RPTJ	Resistivity Permatang Tok Jaya
RTT	Resistivity Titi Teras

SI	Structural Index
SM	Semblance magnitude
UK	United Kingdom
USM	Universiti Sains Malaysia

**TANDA KENAL KEBERINTANGAN 2-D, MAGNETIK DAN RADAR
PENUSUKAN BUMI TERHADAP PENGEBUMIAN MANUSIA YANG
TERJEJAS DENGAN VARIASI MASA DAN JENIS TANAH YANG
BERBEZA**

ABSTRAK

Teknik geofizik banyak digunakan dalam prospek arkeologi untuk mengesan lapisan budaya seperti artifak kuno, pengebumian manusia dan bekas abu. Dalam kajian ini, teknik keberintangan 2-D, radar penusukan bumi dan magnetik telah digunakan untuk mengesan pengebumian manusia. Tempoh pengebumian dan jenis tanah akan menghasilkan tanda kenal anomali yang berbeza. Selain itu, penguraian badan manusia juga akan menjejaskan tanda kenal geofizik. Terdapat empat kawasan kajian yang dipilih iaitu, tanah perkuburan Islam Kampung Permatang Pasir (tanah pasir) terletak di Balik Pulau, Tanah Perkuburan Islam Kampung Titi Teras (tanah lempung berpasir) terletak di Balik Pulau, Kampung Sungai Tokang (tanah lempung) yang terletak di Nibong Tebal dan Kampung Permatang Tok Jaya (tanah pasir lembab) yang terletak di Kepala Batas. Kajian ini menggunakan teknik tinjauan keberintangan 2-D dan tinjauan radar penusukan bumi (GPR) untuk pengimejan 2-D dan 3-D di dalam subpermukaan. Manakala, bagi tinjauan magnetik permukaan, teknik isyarat analitik dan nyahkonvolusi Euler digunakan. Kajian ini bertujuan untuk mengkaji kesan terhadap tindak balas geofizik bagi pengebumian manusia terhadap tahun pengebumian dan jenis tanah yang berbeza. Pengebumian yang baru (<5 tahun) akan menghasil tahap keberintangan yang rendah, 90-580 Ωm dan 300-750 Ωm masing-masing di dalam tanah pasir dan lempung berpasir. Bagi tinjauan GPR, pantulan hiperbola yang jelas dihasilkan dalam tanah pasir dan tanah lempung berpasir.

Pengebumian yang lama (>50 tahun) menunjukkan nilai keberintangan yang sederhana iaitu 400-1000 Ωm di tanah pasir, tetapi nilai keberintangan yang rendah di tanah lempung (2-22 Ωm). Bagi tinjauan GPR, pantulan hiperbola yang sederhana dikesan di tanah pasir lembab, pantulan yang cerah di tanah lempung berpasir dan tanah pasir dan tiada pantulan di tanah lempung. Bagi tanah pasir, nilai keberintangan bagi tanah terganggu adalah lebih rendah berbanding di sekeliling, manakala bagi tanah lempung nilai keberintangan adalah lebih tinggi berbanding di sekeliling. Tinjauan GPR adalah terbaik di dalam tanah pasir dan terburuk di dalam tanah pasir lembab dan lempung. Bagi tinjauan magnetik pula, isyarat analitik medan magnetik tidak dapat menghasilkan resolusi yang terperinci untuk setiap kubur, tetapi tinjauan ini mampu mengesan satu jasad magnetik yang besar. Jangka pengebumian dan jenis tanah akan menghasilkan perbezaan dalam tanda kenal anomali dalam hasil tinjauan keberintangan 2-D, radar penusukan bumi dan magnetik.

**2-D RESISTIVITY, MAGNETIC AND GPR SIGNATURE TOWARDS
HUMAN BURIALS AFFECTED BY TEMPORAL VARIATION AND TYPE
OF SOIL**

ABSTRACT

Geophysical methods are commonly used in archaeological prospect for detecting cultural layer such as ancient artefact, human burials and burnt remains. In this study, 2-D resistivity, GPR and magnetic methods are used to detect human burials. Periods of burial (recent, intermediate and old) and type of soil in burial produced different anomaly signature. Besides, the decomposition of human body will affect the geophysical signature. Four study area were selected which are Kampung Permatang Pasir Muslim cemetery (sandy soil) which located in Balik Pulau, Kampung Titi Teras Muslim cemetery (sandy clay soil) which is in Balik Pulau, Kampung Sungai Tokang (clayey soil) which located in Nibong Tebal and Kampung Permatang Tok Jaya (wet sand) which located in Kepala Batas. In this study, 2-D resistivity and Ground Penetrating Radar (GPR) are used for 2-D and 3-D data subsurface imaging. While for ground magnetic survey, analytic signal and Euler deconvolution technique are used. This study aims to investigate the geophysical response of human burials towards the periods of burial and different types of soil. The recent burials (<5 years) produce low resistivity value of 90-580 Ωm and 300-750 Ωm in sandy soil and sandy clay soil respectively. For GPR method, highly contrast of hyperbolic reflection is produced for both sand and clayey sand soil. While, the old burials (>50 years) show medium resistivity value of 400-1000 Ωm in sand soil, but low resistivity values in clay soil (2-22 Ωm). For GPR survey, medium hyperbolic reflection is found in wet sand soil study area, strong reflection in clayey sand and

sand soil and no reflection in clay soil. For sandy soil, the resistivity value for disturbed soil is lower than surrounding while for clayey soil, it is higher than the resistivity of surrounding. GPR survey is optimum in sandy soil while poor correlation in wet sand and clay soil. For magnetic survey, the analytic signal of magnetic field is unable to provide a detail resolution for each grave, but the method could locate a large magnetic body. The periods of burial and types of soil will produce different anomaly signature on 2-D resistivity, GPR and magnetic result.

CHAPTER 1

INTRODUCTION

1.1 Preface

Geophysical methods have been widely used in various applications such as mineral exploration, groundwater study and engineering purposes. Moreover, geophysical methods are used to detect cultural layer such as buried objects and subsurface structures without damaging the surrounding and target object. Cultural layer is the deposition of materials from settlements of other prehistoric areas of activity that accumulate over a relatively continuous time (Kipfer, 2000).

In archaeological study, 2-D resistivity method has been used to detect subsurface object such as human burials by detecting the disturbed soil cause by the digging process for human burials (Nero et al., 2016). While for the magnetic method, it is used to detect the burnt effect for a long time ago. Besides, the magnetic method also can be used as forensic search tool such as buried weapon and unmarked grave (Pringle et al., 2015). Besides, Ground Penetrating Radar (GPR) method can be used to detect unmarked graves and the result based on the different conductivity and dielectric within the study area (Hansen et al., 2014).

There are variety ways of human burials around the world depending on religion and culture of a civilisation. In Malaysia, dead body will be buried beneath the ground around 2 m depth depending on the type of soil. In some cases, dead body was buried with coffin. Once the body buried, it will undergo decomposition process where on the first three days, the body is still in fresh phase. After three days, the body will start bloating and this process may happen up to 2 weeks to fully bloated stage. After a month, the body will start decay where the body will release fluid and gasses to surrounding soil. These two components will affect the properties of soil. After a

year, the bone will be exposed but the bone is still wet because of decomposition fluid and some tendon still exist within the bone. In 5 years or more, the bone will dry where the effect of decomposition fluid was disappeared and the pH value for the soil will return to original level (Goff, 2009) and the bone breakdown process will start. According to Janaway et al. (2009), the depositional environment will affect the rate of decomposition and the preservation of body is better in deeper condition.

In this study, resistivity, magnetic and GPR methods are used to identify the signature of these geophysical parameters by contrasting age of burials and type of soil of the burials locations. The result will be correlated to enhance the data and increase the probability of finding human burials beneath the subsurface. All the three methods are non-destructive; hence the burials body will be preserved.

1.2 Problem statement

Malaysia is a developing country and a lot of land had been occupied and developed for residential areas and others. Since the number of citizen are increasing with time, the number of death are also increasing. Nowadays, the cemetery is increasingly designated as full and therefore identifying unoccupied space are very crucial for new burials. This is to make sure that new deceased can be properly buried in systematic ways. In previous time, some people buried their deceased family and relatives at their own piece of land which commonly be placed behind their houses. This isolated graveyard in time need to be removed due to development or road expansion. Hence, the isolated old graveyard need to be relocated and centralised by authorities due to development or construction project. Since Malaysia is categorized in tropical region, there are variety type of soils around Penang state. Some cemetery are in sand, clayey sand and clay soils where the burials within this different soils will

produce different signature. Besides, the periods of burial also influence in the different signature of the burial.

Geophysical method is known as effective method to detect the signature of the burials as geophysical methods are non-destructive and cost save. However, there are limitation for each method because of they are totally site dependent.

1.3 Objective

The aims of the study are:

- a) To investigate the effect of period of burials on the 2-D resistivity, GPR and magnetic anomaly signature.
- b) To determine the effect of type of soils towards the ability of 2-D resistivity, GPR and magnetic methods in detecting human burials.
- c) To propose the optimum geophysical method based on the types of soil of target area and periods burial for detecting target.

1.4 Scope of study

Three geophysical methods which are 2-D resistivity, GPR and magnetic methods were used at several locations in Penang state to detect human burials. There are four study areas in this research, two in main island of Penang which are Muslim cemetery in Permatang Pasir and Muslim cemetery in Titi Teras while the other two are unmarked grave in Nibong Tebal and isolated old grave in Permatang Tok Jaya. 2-D resistivity, GPR and magnetic methods were carried out to obtain geophysical responses of the burials. This research focus on three periods of burial which are; recent (< 5 years), intermediate (5-50 years) and old (> 50 years). This research also covers burials in four type of soils which are sand, clayey sand, clay and wet sand.

1.5 Significant of study

This research aims to differentiate the geophysical signature towards human burials in contrasting age of burials and type of soils. The result of this study can be used in locating human burials in different type of soils and different period of burials in Malaysia. This research can help in locating ancient burials for protecting the archaeological cultural relics which will benefit the heritage and tourism sector. Besides, the finding from this study could be used as a guide in locating recent burials for criminal or murder cases and natural disaster.

1.6 Layout of thesis

Basically, the layout of this thesis is as follows:

Chapter 2 explains on the theories behind the three methods which are 2D resistivity, GPR and magnetic methods. Previous study related to age of burials, type of soils and rate of decomposition of human bodies are reviewed for better understanding of the research topic.

Chapter 3 explained the study areas in detail. There are four study areas which are Permatang Pasir, Titi Teras, Nibong Tebal and Permatang Tok Jaya. This chapter also explained about the procedure of the geophysical methods used. The classification of the age of burials also explain in this chapter.

Chapter 4 described about the result obtained for all study areas. The results from 2D resistivity, GPR and magnetic methods are displayed in this chapter. The anomalies are labelled for all line and interpreted. The 3D resistivity and GPR model are displayed to enhance the locality of the anomalies. The intergration of all geophysical methods is explained in detail for each study area. Resistivity values range and reflectivity coefficient and contrast in GPR are extracted from recent, intermediate

and old graves in different type of soils. Then, the graphs and table for these values are displayed in this chapter.

Chapter 5 concluded the whole research to achieve the objective of this research. Some recommendation also discussed to improve the further research quality.

CHAPTER 2

LITERATURE REVIEW

2.1 Introduction

In archaeological prospect, the geophysical studies can contribute a lot of benefits such as low cost, environment preservation and non-destructive method. Human burials can be found at any places which contain of different type of soil and different periods of burial. In geophysical studies, the changes of soil characteristic will affect the reading of 2-D resistivity, GPR and magnetic during the data acquisition. The decomposition process will affect the changes of characteristic thus cause changes in geophysical data. However, the soil properties will affect the rate of decomposition. In terms of age of burials, the body in recent burials is still intact but the decomposition process is already start and the body will be releasing gases and fluid that affect the surrounding. The intermediate burials usually contain wet bone with some flesh remain such as tendon. The released decomposition fluid and gasses from decomposing body will produce changes in soil characteristic. The old burials only contain dry bone where the process of bone breakdown is started. As the burials is old, the effect of soil compaction, small size of skeletonized remains, depth of burials and small relative dielectric contrast between the remains and the surrounding soil will cause slight changes in geophysical data. This will cause difficulty in detecting human burials (Molina et al., 2015).

The rate of decomposition of human bodies are affected by type of soil. Clay soil provide best condition for remains preservation. The soil properties such as permeability and porosity will affect the rate of decomposition. The rate of decomposition will determine the ability of geophysical method to detect human burials. The best preservation in a certain type of soil will produce a clear result in

geophysical result. The faster decomposition rate will cause bone to disappear quickly and cause no changes in geophysical result due to the remain is decayed completely.

2.2 2-D resistivity

The purpose of electrical survey is to measure the resistivity distribution beneath the subsurface by calculating measurements on the ground surface. From these measurements, the true resistivity of subsurface can be estimated. The ground resistivity is related to various geological parameters such as the mineral and fluid content, porosity and degree of water saturation in the rock (Loke, 1999). When two current electrodes are planted into the ground, the current will flow through the earth. The lines of current flow are always perpendicular to the surfaces of potential field where it is always constant or called equipotential field. Figure 2.1 shows the flow of current in the homogenous ground. The potential difference or voltage is a resultant of interaction between the source that drive current through the resistive medium and the subsurface geoelectrical structure (Dobrin and Savit,1988).

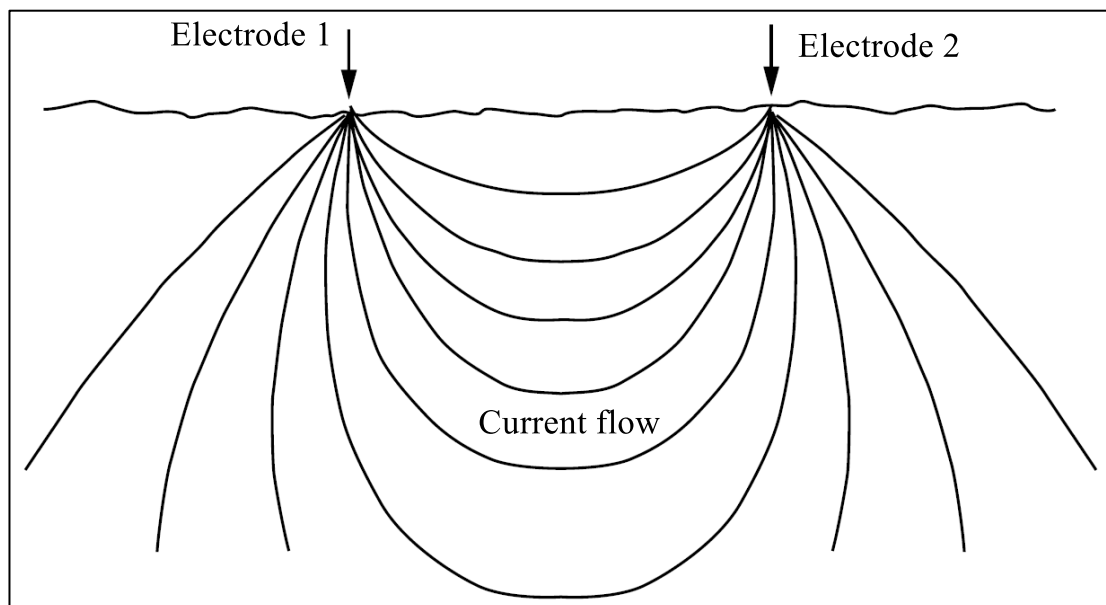


Figure 2.1 Current flow in homogenous ground (Milson, 2007).

In resistivity method, current is introduced into the ground by using two current electrodes (C_1 and C_2) and the resulting potential differences are measured on the surface through two potential electrodes (P_1 and P_2). The arrangement of the electrodes is shown in Figure 2.2.

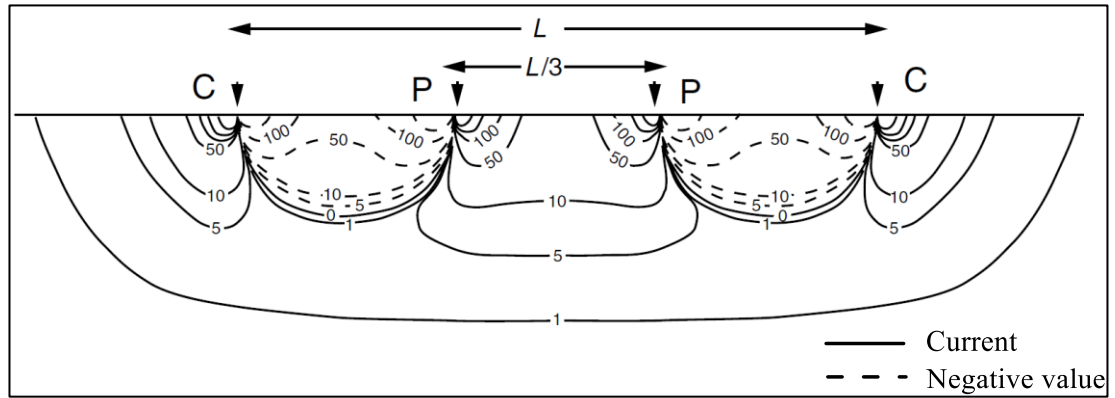


Figure 2.2 Arrangement of electrodes (Milson, 2007).

The voltage, current and resistance can be expressed as in Equation 2.1 where the voltage, V is directly proportional to current, I and resistance, R . Consider current is being supplied to a long wire having a length, L and a cross-sectional area of A , hence resistance can also have written as Equation 2.2 where ρ is resistivity. From the Equation 2.2, the resistivity value can be calculated by substituting the resistance into Equation 2.1 producing new Equation 2.3.

$$V = IR \quad (2.1)$$

$$R = \rho \frac{L}{A} \quad (2.2)$$

$$V = I\rho \frac{L}{A} \quad (2.3)$$

In resistivity method, the recorded resistivity is not the true resistivity value of subsurface, but it is an apparent resistivity, ρ_a which will give the same resistivity value for the same electrode arrangement. To determine the true subsurface resistivity, an inversion of measured apparent resistivity values need to carry out by using a

computer program (Loke, 2000). The apparent resistivity can be expressed in Equation 2.4:

$$\rho_a = k \frac{V}{I} \quad (2.4)$$

Where k is geometric factor, which depends on the arrangement of the four electrodes.

2.2.1 Pole dipole electrode array

There are several arrangements or electrode arrays that have been used in resistivity survey method. The arrays have different characteristics in terms of signal strength, data coverage horizontally, horizontal and vertical sensitivity in changes of the subsurface resistivity and investigated depth. Hence, the maximum depth of target and the interest of the survey determine which array is the best to choose. According to Loke (1999), the best array is depending on the type of structure to be mapped, background noise level and resistivity meter sensitivity. The most commonly used array electrical resistivity survey is Wenner, Dipole-dipole, Wenner Schlumberger, Pole-pole and Pole-dipole. However, this section will only focus on Pole-dipole array which was used in this study. Pole-dipole array use four electrodes, two potential electrodes and two current electrodes, 'a' is spacing between P₁ and P₂ which move along the survey line for 'n' spacing from current electrode C₁. The C₂ electrode act as a remote electrode which must be placed sufficiently far from the survey line. Pole-dipole array is not as sensitive to telluric noise as the Pole-pole array. Pole-dipole array has relatively good horizontal coverage, but it has a significantly higher signal strength compared with Dipole-dipole. Pole-dipole array produces asymmetric anomalies that are consequently more difficult to interpret than those produced by symmetric arrays (Milson, 2007). To eliminate the effect of asymmetry resistivity section, measurements

were repeat with the electrodes arranged in reverse manner and combining the forward and reverse measurement to produce final section.

2.3 Ground Penetrating Radar (GPR)

Ground penetrating radar (GPR) is a non-destructive technique of imaging shallow soil and ground subsurface using electromagnetic (EM) wave. The advantages of using GPR method is the short wavelength of EM wave can be generated and radiated into the ground to detect the anomalous variations in dielectric properties of the geological material (Sharma, 1997). The principle of GPR method is similar to the principle of seismic reflection and sonar surveying. A short radar pulse is radiated into the ground in frequency of 10-1000 MHz and reflected by the subsurface anomalous. GPR method has its own limitation which is high electricity conductivity medium such as damp clay and salt water will limit the penetration and the energy of EM wave will dissipate. On the other hand, the GPR method produces good results in regions of ice, snow, dry soil and over concrete. A GPR system consists of three main components which are transmitter and receiver antenna and a control unit system. The transmitter antenna radiates short EM pulse into the ground where it will be refracted, diffracted and reflected by the medium with contrast in dielectric permitivity constant and electrical conductivity. The basic mechanism of GPR system is shown on Figure 2.3.

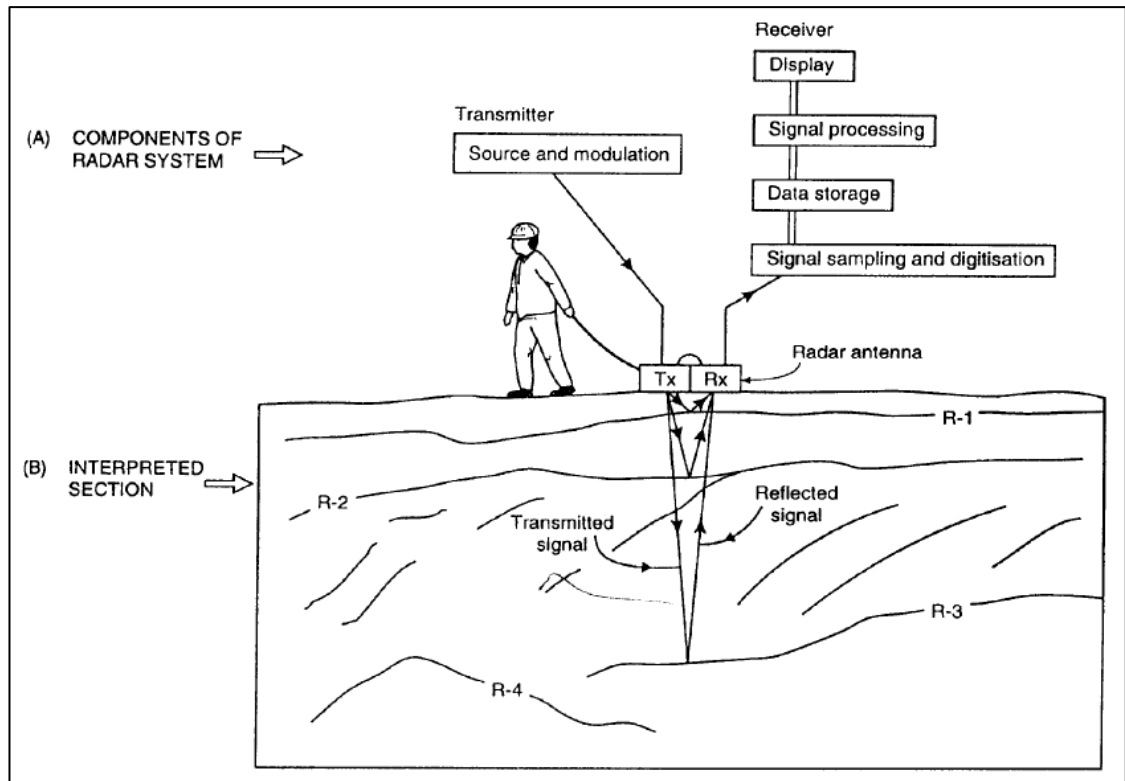


Figure 2.3 Simplified diagram of (A) the constituents of a radar system with (B) the interpreted section (Reynolds, 2011).

2.3.1 Reflectivity

GPR transmitter antenna transmit a very short electromagnetic pulse into the ground and the sudden changes in dielectric properties cause EM wave to be reflected to receiver antenna, recorded and amplified. The recorded signal is registered as amplitude and polarity versus two-way travel time known as radargram

EM wave propagates at speed of light (0.3 m/ns) in air and decreasing when enter a new medium such as ground, water and new layer. The velocity of EM wave in a host medium is given by Equation 2.5:

$$v = \frac{c}{\sqrt{\epsilon_r \mu_r \frac{1 + \sqrt{1 + (\sigma/\omega\epsilon)^2}}{2}}} \quad (2.5)$$

where c is the EM wave velocity in vacuum (0.3 m/ns), $\epsilon = \epsilon_r \epsilon_0$ the dielectric permittivity and ϵ_0 the dielectric permittivity in free space (8.854×10^{-12} F/m), $\omega = 2\pi f$ the angular frequency, where f is the frequency and expression $\sigma/\omega\epsilon$ is a loss factor. The velocity of EM waves is reduced in the non-magnetic low-loss materials (gravel and clean sand) given by Equation 2.6:

$$v = \frac{c}{\sqrt{\epsilon_r}} \quad (2.6)$$

The dielectric contrast between two adjacent medium will cause EM waves reflection known as reflection coefficient (R_c) given in Equation 2.7:

$$R_c = \frac{\sqrt{\epsilon_2} - \sqrt{\epsilon_1}}{\sqrt{\epsilon_2} + \sqrt{\epsilon_1}} \quad (2.7)$$

where ϵ_1 and ϵ_2 are the dielectric constants of two media (or layers) respectively (Reynolds, 2011). The larger the dielectric contrast, the higher the reflectivity coefficient and the clear the target object. Table 2.1 lists the bulk dielectric constant values of common earth materials reported by Cardimona, (2002).

Table 2.1 Bulk dielectric constants of common earth materials (Cardimona, 2002).

Material	Typical dielectric constant	Radar propagation velocity (m/ns)
Air	1	0.30
Water	81	0.033
Granite	9	0.10
Limestone	6	0.12
Sandstone	4	0.15
Rocks	4-12	0.15-0.087
Dry sand	4-6	0.15-0.12
Wet sand	30	0.055
Dry clay	8	0.11
Wet clay	33	0.052
Dry soils	3-8	0.17-0.11
Wet soils	4-40	0.15-0.047
Asphalt	3-6	0.17-0.12
concrete	9-12	0.10-0.087

2.4 Magnetic

Magnetic method is one of the easiest and inexpensive methods compared with the other geophysical method. Magnetic method and gravity method are merely the same in the field technique and the data interpretation. The magnetic method can be applied from the small scale environmental, engineering and archaeological surveys to large scale surveys for investigating regional geological structures (Sharma, 1997).

The principle of magnetic method operation is when a ferrous material is placed within the Earth's magnetic field, it will be induced and then develop induce magnetic field. The magnetic anomaly appeared when the induced magnetic field is superimposed on the Earth magnetic field at certain location. The amount of magnetic material present and the distance from the sensor are the factors of the detection (Rivas, 2009).

2.4.1 Proton precession magnetometer

The most commonly used magnetometers in both base and mobile modes are proton magnetometer. The sensing element consists of a bottle surrounded by a coil of copper wire containing a low freezing-point hydrocarbon fluid. The proton precession magnetometer is using the small magnetic moment of the hydrogen nucleus (proton). When a polarizing current passed through the coil, creating a strong temporary magnetic field, along which the moments of the proton in the hydrogen atoms will tend to become aligned at a large angle of earth's magnetic field. When the current is switched off, the returning of the protons to their original position cause a short precession around the direction of the earth's ambient field. The precession frequency, f is proportional to total field strength can be expressed as Equation 2.8.

$$f = \frac{\gamma_p B_e}{2\pi} \quad (2.8)$$

where γ_p is the gyromagnetic ratio of the proton and B_e is the original alignment of earth magnetic field. Figure 2.4 shows the concept of proton magnetometer.

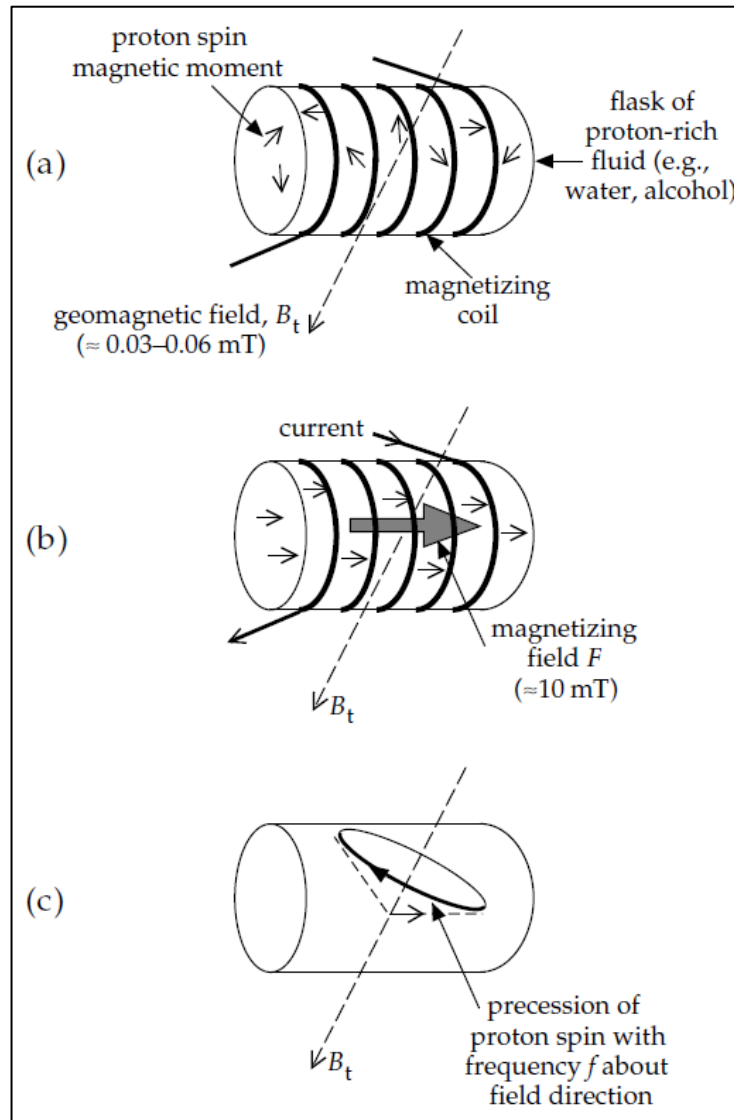


Figure 2.4 The concept of proton precession magnetometer where a) the elements of proton precession magnetometer, b) current in magnetizing coil produces a strong field that aligns the magnetic moments and c) the proton spins precess about the geomagnetic field inducing an alternating current in the coil (Lowrie, 2007).

2.4.2 Filtering

In this study, analytic signal is used to obtain better data interpretation. Analytic signal has property that generates a maximum directly over discrete bodies as well as their edges. Analytic signal is the combination of the horizontal and vertical gradients of the magnetic anomalies (Ansari and Alamdar, 2009). The analytic signal filter has been used for edge detection and depth estimation of magnetic bodies. The filter generated a maximum value directly over the causative body and estimated depth of magnetic bodies. The amplitude of the analytic signal of the total magnetic field, F is calculated from three derivative components of the field and defined as the square root of the squared sum of the vertical and horizontal derivatives of the magnetic field as in Equation 2.9:

$$|A(x, y)| = \sqrt{\left[\left(\frac{dF}{dx}\right)^2 + \left(\frac{dF}{dy}\right)^2 + \left(\frac{dF}{dz}\right)^2\right]} \quad (2.9)$$

Where A is the amplitude of the analytic signal and F is the measured total magnetic field. In this study, the derivative components are calculated by applying derivative filter on the total magnetic field. Then, analytic signal is obtained by using the formula. The advantage of analytic signal is the amplitude function is always positive and does not any assumption of the direction of body magnetization (Jeng et al., 2003).

In this study, Euler deconvolution method is used to obtain boundary and depth of magnetic bodies. The information about magnetization vector are not required and it only need a little prior knowledge about the magnetic source (Thompson, 1982). This process is done by applying Euler's Homogeneity (Equation 2.10) as the following.

$$(x - x_0) \frac{dF}{dx} + (y - y_0) \frac{dF}{dy} + (z - z_0) \frac{dF}{dz} = N(B - F) \quad (2.10)$$

where x_0 , y_0 and z_0 are the source locations which the magnetic field F , measured at x , y and z_0 , B is the regional value of the total magnetic field, N is the Structural Index (SI) which characterizes the source geometry. The most crucial in Euler deconvolution is the N (SI). By changing N , the geometry and depth of magnetic source can be estimated. A poor choices SI will give a diffuse solution of source location and a deviation of depth estimation. A correct N gives the tightest clustering of the Euler solutions around the geologic structure of interest (Reid et al.,1990).

2.5 Temporal variation

Jervis et al. (2009) conducted a time-lapse resistivity survey study in clandestine graves. The aim of this study was to develop a better understanding of how electrical resistivity surveys can be used to locate clandestine graves. Three simulated clandestine graves containing a pig cadaver, no cadaver and a pig cadaver wrapped in tarpaulin were constantly undergo resistivity survey. In the survey data (Figure 2.5), the grave containing a pig cadaver was detectable from a low resistivity anomaly(-3 Ωm). From groundwater data, it is suggested that the resistivity anomaly associated with the surveyed pig grave was caused by a localised increase in groundwater conductivity. The wrapped pig cadaver produced high resistivity response (3 Ωm) due to the tarpaulin prevented the decomposition fluid from mixing with the surrounding. The disturbed soil in empty grave was not detected by the resistivity survey. Although soil samples showed grave soil to be more porous than undisturbed soil, the lack of response from the grave that did not contain a cadaver suggests that disturbed soil was not responsible for the resistivity anomalies observed in this study. Resistivity surveys successfully detected all graves containing cadavers throughout the study, whilst also showing the potential to eliminate the need for mass excavation in a genuine search.

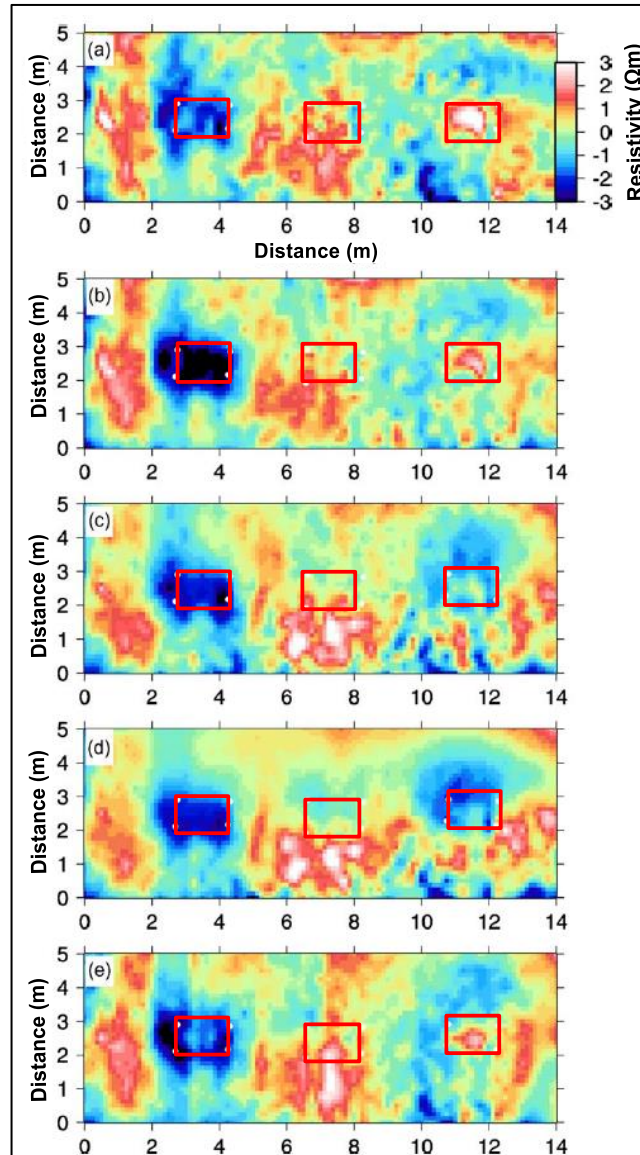


Figure 2.5 Result of processed and normalised resistivity survey (a) 28 days after burials (b) 140 days after burial (c) 192 days after burial (d) 252 days after burial (e) 364 days after burial. The edges of each graves are marked by red box (Jervis et al. 2009)

Pringle and Jervis (2010) conducted a research about electrical survey to search for a recent clandestine burial of a homicide victim in UK. The objective of this study was to assist the search for a suspected 1-year-old clandestine burial of a murder victim in North Wales in the UK. The conventional search techniques such as victim recovery dogs and probing were unsuccessful, and a high clay content soil limit the GPR method as study method, hence a resistivity survey was instead trialled. Ten resistivity grids

were conducted and site detrended with user-specified, contoured anomalies being generated. The anomalies detected in the result were compared to anomalies derived from similar-aged and simulated clandestine burial surveys where the simulated naked pig burial produce $-3 \Omega\text{m}$ and wrapped pig burial produce $3 \Omega\text{m}$ (Figure 2.6). This value is used to detect potential burials by comparing with the resistivity result in real burial sites. Several locations with low resistivity are assumed as potential burials location which is suspected to be 1-years burials (Figure 2.7).

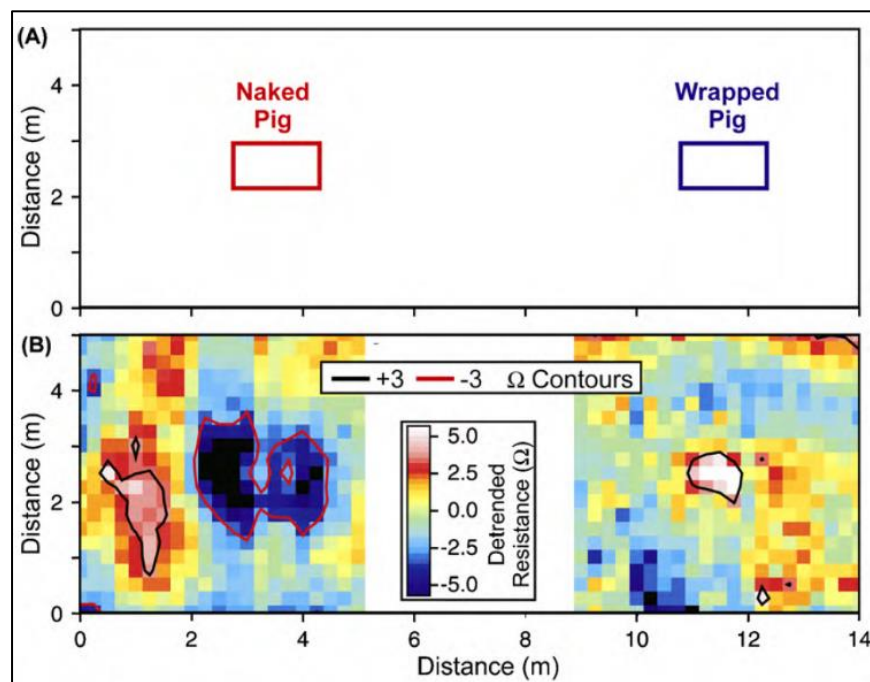


Figure 2.6 Bulk ground resistivity data over simulated clandestine graves. a) location of burials, b) resistivity data result (Pringle and Jervis, 2010).

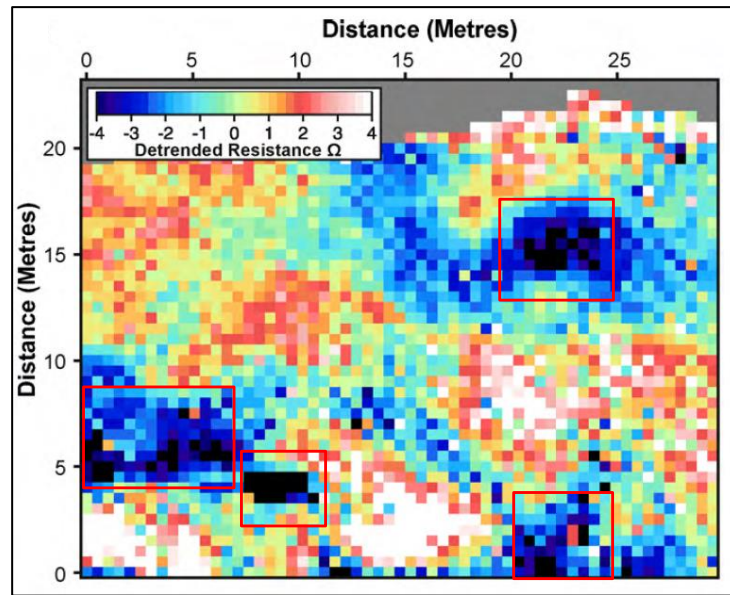


Figure 2.7 Processed bulk ground resistivity plan view where the red box indicates the potential burials location (Pringle and Jervis, 2010).

Booth and Pringle (2016) conducted a research focusing on GPR survey for forensic search. The research is about semblance analysis to assess GPR data from a five-year forensic study of simulated clandestine graves. The research goal was to develop a semblance-based method to quantify the assessment of a time-lapse archive of GPR. This study uses a common-offset configuration of semblance analysis to characterise velocity trends from GPR diffraction hyperbolae and to quantify the strength of GPR response since the magnitude of a semblance response is proportional to signal-to-noise ratio. 2D GPR profiles were acquired over two simulated clandestine burial which were wrapped-pig cadaver and naked pig cadaver were monitored for every three months between 2008 to 2013 by using three different GPR antennas which were 110 MHz, 225 MHz and 450 MHz. The GPR response for the cadavers was a hyperbolic structure. As a result, the semblance analysis has little sensitivity to changes attributable to decomposition, and only a subtle influence from seasonality where velocity increases about 0.01 m/ns to 0.02 m/ns were observed in summer, associated with a decrease (5–10%) in peak semblance magnitude, SM, and potentially in the

reflectivity of the cadaver. The lowest frequency antennas consistently gave the highest signal-to-noise ratio although the grave was nonetheless detectable by all frequencies trialled. These observations suggest that forensic GPR surveys could be undertaken with little seasonal hindrance. Whilst GPR analysis cannot currently provide a quantitative diagnostic proxy for time-since-burial, the consistency of responses suggests that graves will remain detectable beyond the five years (Figure 2.8).

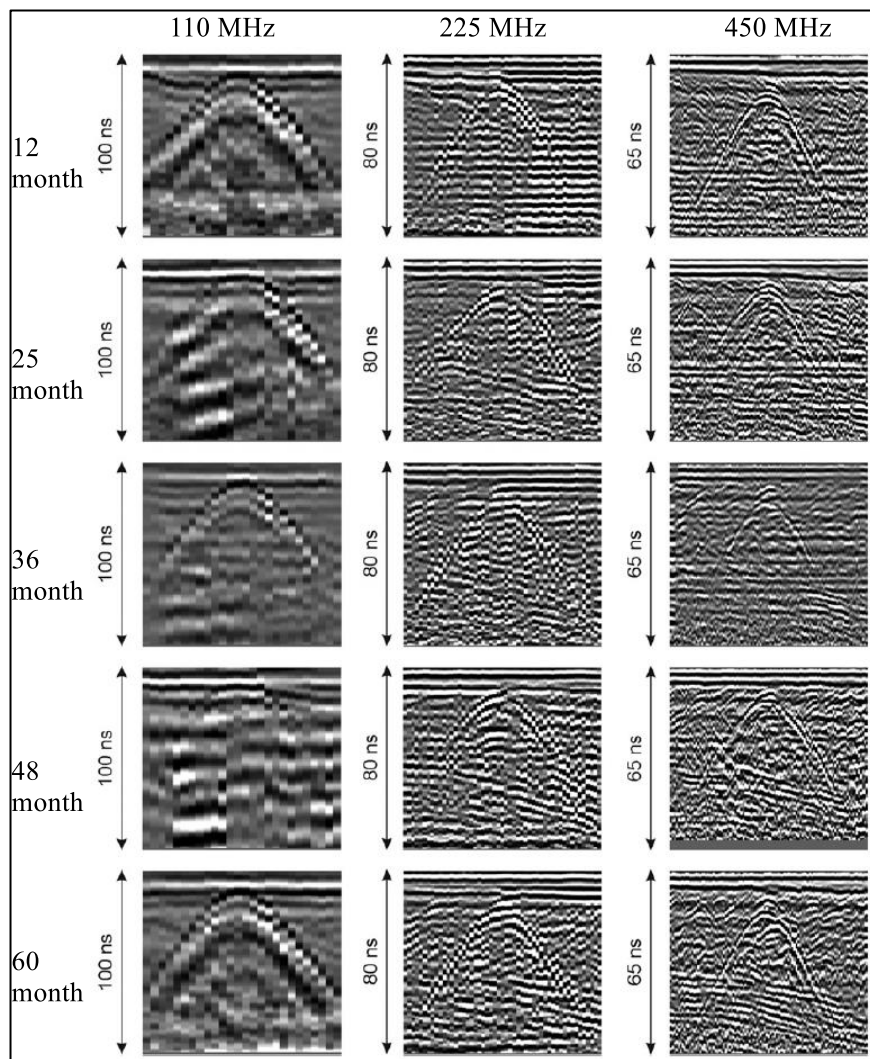


Figure 2.8 GPR 2D profile for 110, 225 and 450 MHz in 12, 24, 36, 48 and 60 months after burials (Booth and Pringle, 2016).

Epov et al. (2016) were conducted a study of integrated archaeological and geophysical studies in West Siberia. This paper presented the most informative results

of archaeological and geophysical field studies of the Baraba forest–steppe over the last three years. The study aims to optimize methods of archaeological and geophysical research. The studies were carried out at the different types belonging to a wide time interval (~6000 BC–2000 AD) of archaeological sites. By using magnetic and electrical method, the data on the presence, size, and configuration of archaeological objects could be obtained. The contrast between the magnetic properties of the upper horizon of present-day soil and underlying substratum at archaeological sites of different types and ages was studied. Magnetometry loses its efficiency with the low contrast between magnetic susceptibility of the filling of archaeological sites and the host medium. The low contrast reduces amplitudes of magnetic anomalies above buried ancient structures. This research show that vertical derivative of magnetic method provides detailed information of the historic burial while electrical method is less effective in detecting burials (Figure 2.9).

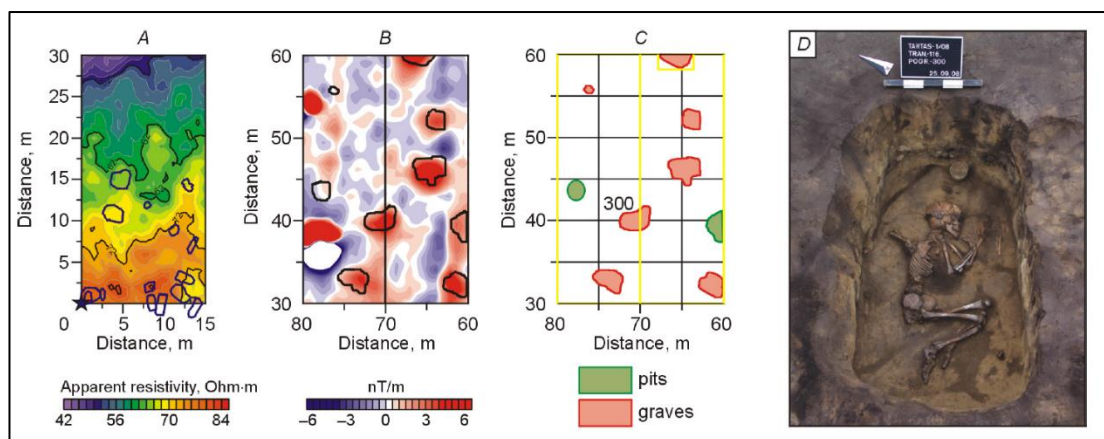


Figure 2.9 Result of geophysical methods which are a) map of resistivity distribution, b) detailed elaboration of vertical derivative of magnetic induction vector modulus, c) map of graves and pits and d) excavation result of a grave (Epov et al. 2016).

Büyüksaraç et al. (2014) conducted geophysical investigation at Agadere Cemetery, Gallipoli Peninsular, NW Turkey. This study aims to explore buried graves

by using GPR, electrical resistivity tomography (ERT) and magnetic imaging (MI). These burials existed since 1915 (99 years old when this study was conducted). In this study, measured apparent resistivity data were processed using a 2D tomographic inversion (Figure 2.10). The high resistivity (20-24 Ωm) anomalies are located between the horizontal distance of about 27-47 m. Resultant resistivity depth slices and volumetric resistivity images clearly showed the anomaly zone, which may be attributed to anthropogenic burials. In GPR (Figure 2.11), the anomaly zones cause reflection due to the material filled voids and suggested that the decomposition of bones may result in calcium salts being leached into the surrounding soil. MI data were processed using linear transformation and an analytic signal image map presented anomaly zones located in some parts of the area (Figure 2.12). Analytic method produces clear anomalous zones (debris, pits and man-made buried structure) Results derived from data processing techniques showed that these methods are suitable for bordering the locations of other buried historical graves in areas that have the same geological environment in the Peninsula.

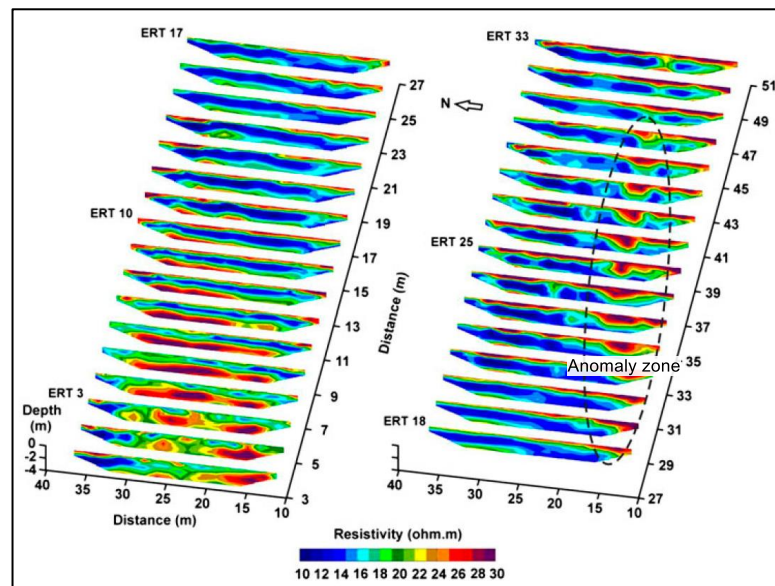


Figure 2.10 Electrical resistivity tomograms (Büyüksaraç et al. 2016).

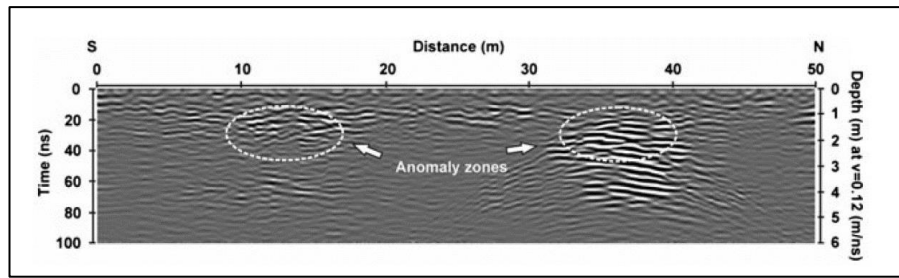


Figure 2.11 2D GPR profile (Büyüksaraç et al. 2016).

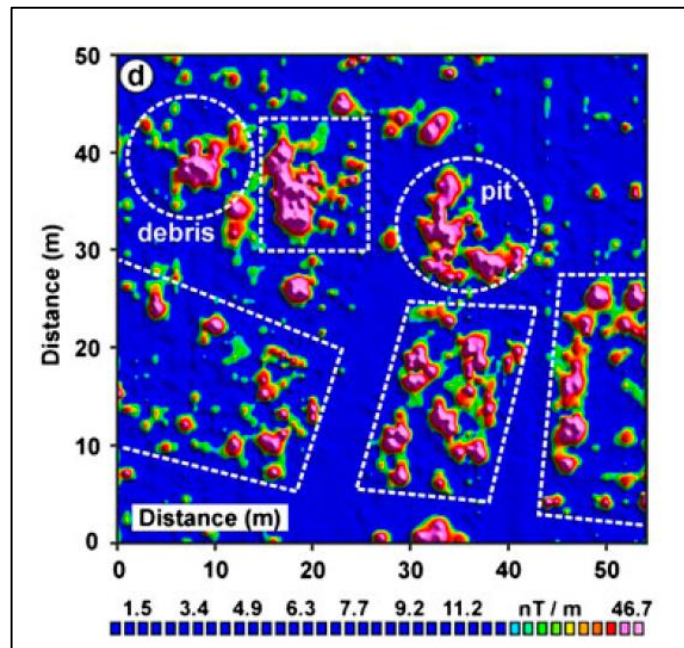


Figure 2.12 Analytic signal of the anomaly marked with white dotted (Büyüksaraç et al. 2016).

2.6 Effect of different types of soil

Hansen et al. (2014) conducted GPR and bulk ground resistivity surveys in graveyards to locate unmarked burials in contrasting soil types. There has been a lack of research to-date on optimal methods and/or equipment configuration of non-invasive geophysical method. By using GPR survey with 225 MHz frequency antenna of 0.25 m spaced profile, the unmarked burials in these case studies that were not uniform or predicted could be effectively identified. Bulk ground electrical surveys, rarely used for unmarked burials, revealed 1 m probe spacings were optimal compared to 0.5m, with datasets needing 3D detrending to reveal burial positions. Results were

variable depending upon soil type; in very coarse soils GPR was optimal; whereas resistivity was optimal in clay-rich soils and both were optimal in sandy and black earth soils. The result is summarized in Table 2.2. Archaeological excavations revealed unmarked burials, extra/missing individuals from parish records and a variety of burial styles from isolated, brick-lined, to vertically stacked individuals. This study suggest that evidence unmarked burial targets were significantly different from clandestine burials of murder victims which are used as analogues.

Table 2.2 Summary of GPR and bulk resistivity in contrasting type of soils (Hansen et al. 2014).

Type of soil	GPR	Bulk resistivity
Sandy soil	Optimal	Highly useful
Clay rich soil	Not optimal	Optimal
Black earth soil	Optimal	Optimal
Coarse with pebble	Optimal	Not recommended

Pringle et al. (2012a) established forensic search methodologies and geophysical surveying for the detection of clandestine grave in coastal beach environment. This study aimed to establish relevant forensic search methodologies to aid the search for clandestine coastal burial sites, using the North-West English coastline as a search area. Three prioritised coastal locations were subsequently identified at coastal dunes and beach foreshore. At all locations, simulated clandestine graves were hand-dug by spades into which a naked adult-sized, metal-jointed fiberglass mannequin was buried at 0.5 m below ground level. GPR data showed 450 MHz frequency antennae to be optimal in sand dune site which depth of penetration approximately 2.3 m but significantly poor data obtained from the foreshore area due to saline seawater which depth of penetration approximately 0.9 m. Electrical resistivity and magnetic susceptibility surveys were successful in coastal environments in target detection, with resistivity fixed-offset configurations deemed optimal. The